Detectors for nuclear resonant scattering experiments

Alfred Q.R. Baron
SPring-8, 1-1-1 Kouto, Mikazuki-cho, Sayo-gun, Hyogo-ken, 679-5198 Japan
E-mail: baron@spring8.or.jp

Detectors and electronics for nuclear resonant scattering (NRS) experiments using synchrotron radiation are discussed. An introduction to X-ray timing measurements is given, followed by a historical look at the detectors that have been employed. The bulk of the article discusses silicon avalanche photodiodes (APDs), as these are presently the most commonly used devices. APDs from several manufacturers are discussed, with emphasis on their relative merits.

1. Introduction

Detectors, and the associated timing electronics, are a crucial part of nuclear resonant scattering (NRS) experiments. While early work [1] used a slow Ge diode detector (also a Ge(1 1 1) monochromator), detectors (like optics) have become both more flexible and more specialized. Thus a greater range of experiments can be done, but it is important to choose the proper detector for a particular application. Also, in order to interpret the experimental results, the response of the detector, and of the entire chain of electronics, should be well understood.

This paper is an introduction to the detectors used in NRS measurements, with a strong emphasis on those most commonly used today: avalanche photodiodes (APDs). A discussion of the scheme of the electronics provides a general introduction to the relevant concepts. This is followed by a historical summary of some of the detectors that have been used. Then we go into detail regarding the various types of APDs available and their relative merits.

2. Timing electronics

The main characteristic of most nuclear scattering experiments is that they require a time resolved X-ray measurement. Short ($\sim$100 ps) pulses of synchrotron radiation arrive at the sample at well defined times: repetition rates typically vary from about 0.2 MHz to 10 MHz. Nuclear scattering events are usually separated from background processes (electronic scattering) by gating in time: electronic scattering occurs on a (sub) ps time scale and is **prompt** while nuclear scattering occurs on longer time scales (typically 10's of ns) and is **delayed**. The quantity of interest in experiments is usually either the amount of delayed radiation as a function of some external parameter (e.g.,

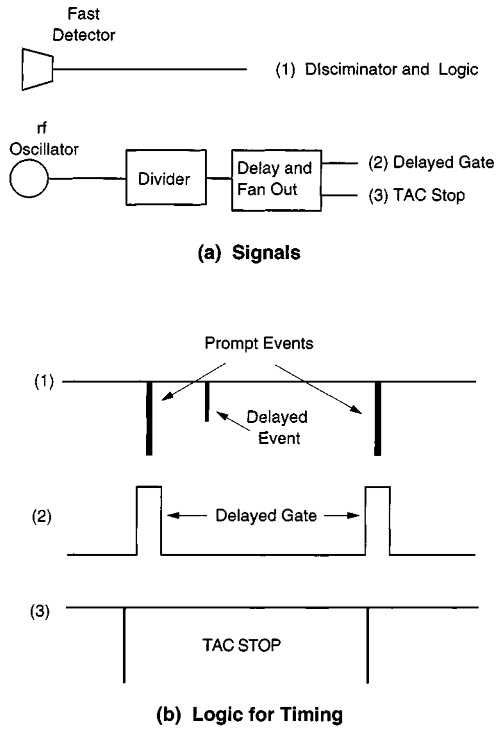

Figure 1. Schematic of the electronics: (a) input signals; (b) logic diagram.

monochromator position or sample temperature), or the detailed time evolution of the delayed radiation after the exciting pulse, or both. In most experiments the amount of nuclear scattering is rather less (say, 4–6 orders of magnitude)[1] than the electronic scattering, so time gating is crucial.

The essential scheme of the electronics for time resolved NRS measurements is shown in figure 1. There are two main input channels, one from the fast X-ray detector and one from the ring timing electronics. The latter is usually derived from the master oscillator controlling the radio-frequency (rf) operation of the storage ring, and is locked to the arrival time of the X-ray pulses at the sample. It is used both to generate a gate to separate delayed events from prompt ones and as the STOP input to the time-to-amplitude converter (TAC) to determine the interval of time between the exciting prompt pulse and delayed event. The use of the ring timing signal as a stop (instead of a start) is to reduce the dead-time of the TAC and necessitates a (trivial) inversion of the time axis for the data.

The overall time resolution of the system is typically between about 100 ps and a few ns. Limiting factors include the synchrotron pulse width, X-ray detector time resolution and the jitter in the electronics. The synchrotron pulse width (the

[1] Exceptions include the use of a crossed polarizer arrangement and pure nuclear reflections. See sections IV-1.1, VI-1 and VII-2 of this issue.

electron/positron bunch length in the storage ring) is typically small, $<$100 ps, though it does depend on the bunch current and can be longer at older machines. The jitter in the electronics is typically also small ($<$20 ps), however, incautious use of delay generators and other modules can increase the jitter. The limiting factor in the overall time resolution is usually the detector at about 1–2 ns, as is discussed below.

Another important time scale for these experiments is that of the gating used to differentiate between prompt and delayed events. Typically the gating is done directly at the discriminator, or using a fast logic box. The gate transition or switching times are of the order of 3–5 ns. However, in high prompt rate experiments (e.g., NFS) it is often the shape of the detector output signal that is the limiting factor. This will be discussed in more detail below, but it means that it is not uncommon for the NFS signal to be only available some 20–30 ns after the prompt pulse. Some trade-offs can be made (better gating performance at the cost of reduced count rate).

Finally, we note that at present, data are taken in histogram or scan form: at the end of the experiment, one has either a collection of histograms of counts versus time, or some scans of delayed counts versus, say, the angle of some crystal. Alternatively, one might consider a nuclear (or high energy) physics data taking format, where each event is individually recorded, providing an event by event list of the time of the event and the other experimental parameters (crystal positions, sample temperatures, etc.). Then, in addition to observing very specific things during the experiment, different binning could be done afterwards, perhaps to highlight or investigate correlations that might not have been thought of before or during the experiment. With the relatively low count rates from nuclear scattering experiments (typically $<$1 kHz) this event by event processing is certainly possible, but, to the knowledge of this author, has not yet been implemented.

3. General considerations for NRS detectors

The specific characteristics required for a detector in an NRS experiment depend somewhat on the application. However, a list of characteristics generally desirable for such detectors includes

1. Good Detector Quantum Efficiency (DQE $>$ 10%, $>$50% preferred).
2. Low background rate ($<$0.1 Hz, $<\sim$0.01 Hz preferred).
3. Good time resolution ($<$10 ns, $<$1 ns preferred).
4. Fast recovery/large dynamic range.

The first two points are desirable in any detector. However, for nuclear scattering experiments, where signal rates can too easily be reduced to $\sim$0.1 Hz, their importance is increased. The second two are more specialized points. Almost all NRS experiments require a time resolution at the 10 ns level, and, depending on the experiment, resolutions of 0.1 ns, or less, can be desired. Faster is generally better, but usually one must make trade-offs (e.g., sacrificing speed for efficiency). Practically, most detectors used have resolutions in the 1–2 ns range. In general, the lower limit of the desired time resolution is set by the pulse width of the radiation from the storage ring. This is typically <1 ns, with the minimum some 10 s of ps, depending on the storage ring and the mode of operation.

The recovery/dynamic range (4th) requirement is very particular to NRS experiments. Its importance depends critically on the prompt count rate. At one extreme, the prompt rate may be much less than the synchrotron pulse rate, perhaps even smaller than the delayed rate (e.g., using crossed polarizers or pure nuclear reflections). In this case, if the detector (and associated electronics) requires a microsecond, or even a few microseconds, to recover after a prompt event, the experiment is not affected because the dead time is small. However, when the prompt rate approaches that of the incident pulses (typical for inelastic absorption measurements – see section V-1.1), the detector must be able to respond quickly or the dead time will be severe. The extreme version of this occurs in nuclear forward scattering (NFS) experiments where each prompt pulse arriving at the detector may contain tens (even hundreds) of photons. Then the detector must recover from a huge pulse quickly to see a single photon some ns later. In this last case, the signal from the detector must be both fast and clean, and all reflections from interfaces of electronics and cables must be removed to prevent reflections and multiple triggering from the huge prompt events.

4. Historical summary of detectors used in NRS

The germanium detector used in the first work [1] was quickly superseded by a plastic scintillator coincidence detector. The use of plastic scintillator improves the time resolution, but the relatively low light output means the signal is not much above that from a single electron thermally emitted from the cathode or early dynodes. Thus, to reduce the noise, a coincidence detector was developed [2]:[2] two photomultiplier tubes (PMTs) look at the same piece of plastic and events are registered only when the output of both PMTs exceeds some threshold simultaneously. This type of coincidence detector was the standard for some years, providing, typically, 1–2 ns time resolution, noise rates of 0.2–3 Hz, and efficiencies of about 35% for 14.4 keV X-rays. However, one serious drawback of such devices (aside from their fairly large size) is that PMTs respond poorly at extremely high count rates. In particular, after-pulsing can occur that then leads to noise in the delayed window. To this author's knowledge, published data from the highest rate experiments was done at count rates of about 1–3 detected photons/prompt pulse (1.8 MHz pulse rate) [3].

The next large step in detector development was the use of silicon avalanche photodiodes (APDs). These directly convert the incident X-ray into e–h pairs, and then provide some internal amplification. They were first used in nuclear scattering exper-

[2] However, a similar detector as in [2] was also developed independently at SSRL by S. Ruby and J. Arthur.

iments by Kishimoto [4] while Ruby noted that large area devices were available [5], making it practical to use APDs in experiments at second generation synchrotron radiation sources. APD detectors are now the standard in most experiments, and will be discussed in some detail below. The main improvements of APDs relative to the plastic detector (aside from the convenience of their smaller size) is their better response at high rates and their lower noise ($<$0.05 Hz).

Other types of detectors have also been considered and developed. Those mentioned above are gated after all gain mechanisms take place (either in the APD or the PMT), but it is certainly possible (and perhaps more sensible) to gate the detector before gain takes place. Preliminary work was carried out along these lines using switched HV supplies with microchannel plates [6] and, more recently, a PMT detector has been developed where the gain is switched on and off by pulsing the dynodes [7].

One may also consider detecting electrons (e.g., from internal conversion) instead of X-rays. Early attempts to see resonant absorption at a synchrotron source used a channeltron electron detector [8]. More recently, a micro-channel plate electron detector has been developed in Hamburg [9] and successfully demonstrated [10]. Presently, some work is also being done to use APDs for direct detection of conversion electrons [11]. Finally, we note that the first incoherent 4π scattering measurements were done using a plastic detector with the sample mounted inside the detector [12], though this detector has been largely superseded by APDs.

5. Avalanche photodiodes (APDs)

Silicon avalanche diodes (APDs) are presently the most frequently used detectors in nuclear scattering experiments. Here we provide a brief introduction to their operation and then discuss some of the APDs that are available. We try to present enough information to understand the basics of APD response to X-rays. A more complete discussion of their structure (doping, fields, gain), may be found in [13] and reviews of Si charge transport may be found in [14,15].

Schematics of the structure of two of the devices commonly used are shown in figure 2. In both cases the depletion layer of the device consists of a low field (drift) region and a high field (gain) region. For modest energy X-rays (say, 4–40 keV) the dominant process in Si is photoelectric absorption, typically leading to a single electron having almost the energy of the incident X-ray. This electron then quickly loses energy to scattering processes in the silicon (typical electron range is $\sim\mu$m). On average, at room temperature, one electron–hole pair will be created for each 3.6 eV of energy deposited in the silicon. Thus, absorption of a single 14.4 keV X-ray will create about 4000 electron–hole pairs in an essentially point-like region of the diode. The electrons drift to the gain region of the device and are amplified.

An essential parameter for X-ray detection is the active thickness of the device: that part of the silicon in which X-ray absorption will lead to subsequent electron amplification. This affects **both** the efficiency of the device and the time resolution.

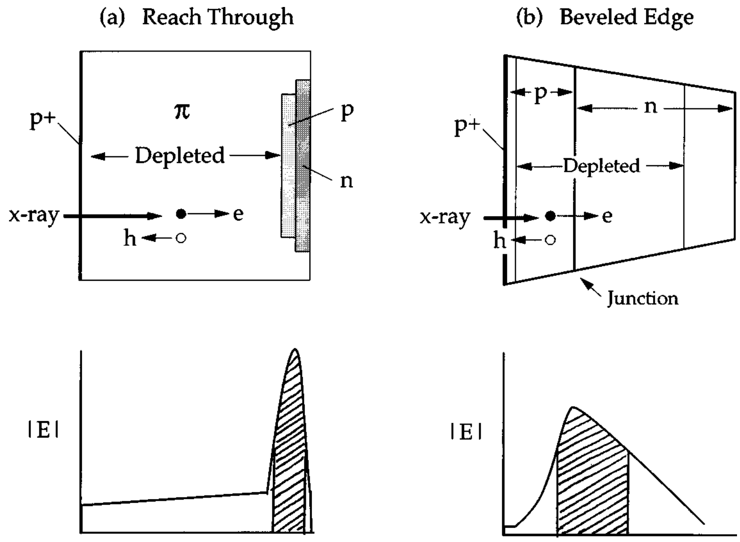

Figure 2. Schematic of diode structures and field profiles. Shaded section of field plot indicates gain region. After [13].

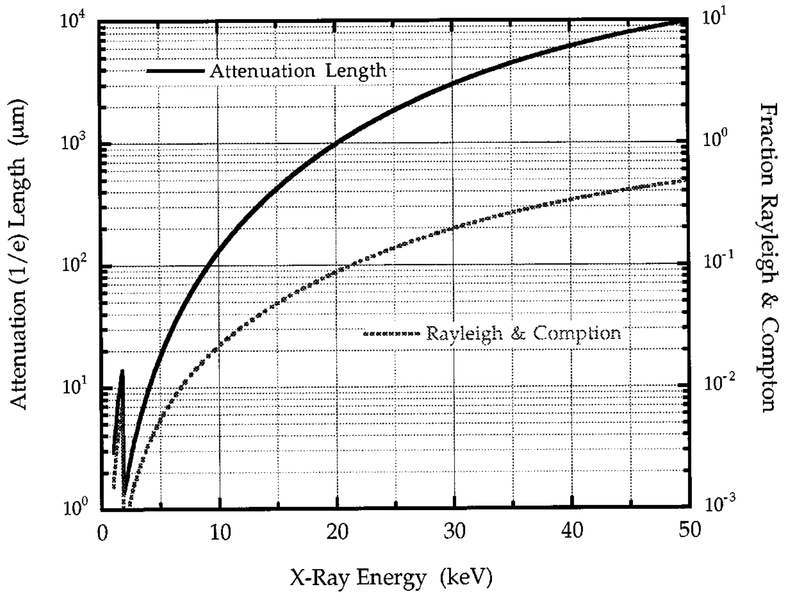

Figure 3. X-ray attenuation (1/e) length in Si and fraction Compton/Rayleigh scattering (Si density = 2.32 gcm^{-3}). This is derived using calculations based on [16] using code based on [17].

The absorption length in Si as a function of X-ray energy is shown in figure 3. As soon as one gets much above 10 keV, it is clear that an active thickness of 100 μm (or more) is desirable to have reasonable efficiency. Meanwhile, the high field drift velocity in Si is only about 100 μm/ns [15]. As X-rays tend to penetrate and (to a first approximation) uniformly illuminate the active thickness of Si, the time resolution is generally not better than the active thickness over the drift velocity. This means there is typically a trade-off between device efficiency and time resolution: for example, a 100 μm thick device will generally not have better than about 1 ns time resolution.

6. APD signal shape

The signal from the APD is amplified by a broad-band (∼GHz) voltage amplifier (see [20]).[3] Typical signal shapes for several diodes are shown in figure 4. APDs with smaller capacitance (smaller area and/or thicker depletion region) will have faster signals. More exactly, considering the APD as a parallel plate device with constant field [18], one finds the rise time of the signal will be governed by the details of the charge transport within the device while the fall time is not better than the RC time constant of the diode capacitance and the amplifier input impedance (e.g., RC = 5 ns for a 100 pF diode capacitance into 50 ohm).

The actual shape of the diode output signal is important for gating out prompt events. If the width of the voltage signal is 5 ns (independent of the time resolution of the APD – which is usually much better), one can not properly discriminate two successive single photon events separated by less than this. In fact, when the prompt rate is very high (e.g., NFS experiments) then the relevant question becomes, given a prompt pulse of say 10 (or more) photons, how long will it take the detector/electronics to recover to detect a single one. More so, for an experiment where one cares about the detailed time structure of the nuclear scattering, the question is really how long one must wait so that the large prompt pulse no longer affects the time at which the discriminator will trigger. Thus, from the point of view of gating, smaller diodes are to be preferred. Practically, using $5 \times 5\ \mathrm{mm}^2$ diodes from EG&G (∼30 pF capacitance), in high rate ^{57}Fe NFS experiments at ESRF, the data is usually available some 20 ns after the prompt pulse. Going to shorter times, particularly if the detailed time response is important, requires special care.

[3] These amplifiers are available from many companies, including Phillips Scientific, and EG&G Ortec, Mincircuits, etc. This type of amplifier was chosen due to a mixture of convenience and speed. If noise is an issue, as it sometimes is for the larger area devices, one might consider reducing the bandwidth, which, in principle should reduce the noise. However, purely as a practical point, commercially available "low noise" medium bandwidth (say, 100–300 MHz) amplifiers do not seem to have much better noise properties than the wide bandwidth (∼GHz) ones. Another possibility would be to use a current (trans-impedance) amplifier instead. However, while high bandwidth trans-impedance amplifiers exist, the author has not noted significant improvement in the signal to noise ratio when they were used, without significant degradation of the time response (fall times of 20 ns or more).

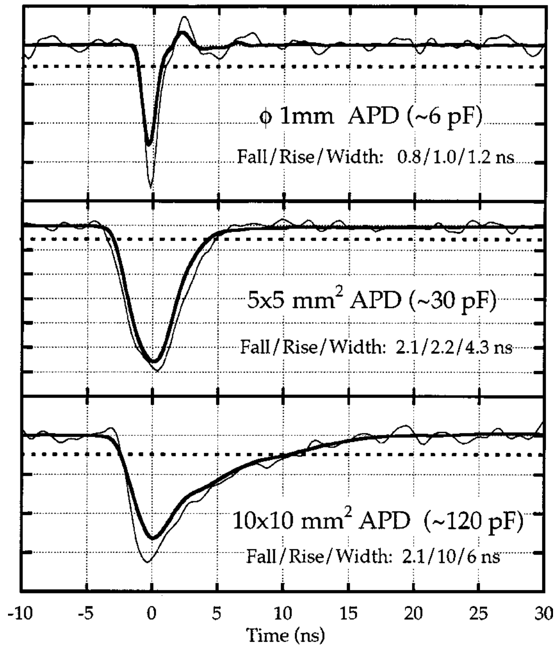

Figure 4. Signal shape from several diodes (1 mm diameter Hamamatsu 2383 and larger area EG&G diodes). Heavy line in each case is the average response while the thin line is a single photon event. Dashed line indicates approximate noise threshold. Waveforms recorded using a 500 MHz, 2GS/s scope (TDS 620) after amplification by a wide bandwidth (∼GHz) preamplifier.

7. Beveled edge APDs

Large area beveled edge devices are available from Advanced Photonix Inc. (API)[4] and Radiation Monitoring Devices (RMD)[5] (see table 1). In general, these devices may have relatively high gains (M $\sim$ 100–1000) and can have exceptionally high gains ($>$10000) [19]. This makes them convenient for detection of lower energy photons. However, the time resolution of the devices, as seen in figures 5(a), (b), is less than ideal for forward scattering experiments. While their FWHM is typically $<$1 ns, they also have a tail to longer times which is caused by the absorption of X-rays in the front, undepleted region of the diode [5]. In the API diodes, the tail extends to $\sim$5 ns and tends to be longer in the RMD devices. However, for inelastic absorption experiments, where one is less concerned with the time response of the sample, this tail is not a major problem. Likewise, while their active thickness (30–50 μm) is a little smaller than desired, it is sufficient for reasonable efficiency at lower energies ($\sim$50% at 6.4 keV).

A serious practical difficulty with the 16 mm diameter API devices, however, is their limited lifetime. In this authors experience, some devices can perform beautifully

[4] Advanced Photonix Inc., 1240 Avenida Acaso, Camarillo CA 93012, USA.
[5] Radiation Monitoring Devices, 44 Hunt Street, Watertown MA, 02172.

Table 1
List of some available APDs. References are to some relevant papers.

Company and type	Area and model	Operating voltage	Active thickness	Time resolution	References
Advanced Photonix Inc.[4] (API) Beveled edge	⌀5, 10, 16 mm (also smaller)	2000–2500 V	30–50 μm	∼0.5 ns FWHM Tail to >5 ns	[5,34–36]
Radiation Monitoring Devices[5] (RMD) Beveled edge	8×8 mm^2 (also custom)	∼1800 V	30–50 μm	∼0.5 ns FWHM Tail to >10 ns	[37,38]
EG&G Optoelectronics[6] Reach-through	5×5 mm^2 (C30626)	300–400 V	∼110 μm	∼1.6 ns FWHM Tail to ∼5 ns	[20] [39–41]
	10×10 mm^2 (C30703)	350–450 V	∼110 μm	∼0.7 ns FWHM Tail to ∼4 ns	[21]
	10×10 mm^2 (Prototype)	350–450 V	∼185 μm	∼1.7 ns FWHM Tail to ∼5 ns	[24]
Hamamatsu Photonics[7] Reach-through	⌀ 1, 3, 5 mm (S238X)	100–250 V	∼30 μm	∼0.3 ns FWHM, Tail to >5 ns	[4]
	⌀ 1, 3, 5 mm (S534X)	∼150 V	∼10 μm	∼0.1 ns FWHM Tail <2 ns	[22]
	⌀ 1, 3, 5 mm (S534X LC)	250–300 V	∼25 μm	∼0.2 ns FWHM Tail <2 ns	[24]
	⌀ 3 mm	∼700 V	∼130 μm	∼1.3 ns FWHM	[23]

for more than 1000 h while others will suffer a serious and irreversible increase in dark current (making them unusable) minutes after the HV is turned on: APD lifetimes vary from minutes, to days to months. One also notes that not all devices have high gain, so sometimes 6.4 keV detection can be difficult. The RMD devices tend to have higher gain and, in this author's experience (4 diodes, 8×8 mm^2 tested for, perhaps, 100 h each) do not die irreversibly. However, they do sometimes suffer dark current increases, which are reversible on baking (120°C for about a day). These dark current increases may be due to moisture absorption and, thus, might be avoided by keeping them in a dry atmosphere.

8. Reach-through APDs

Reach-through devices are available from both Perkin–Elmer (formerly EG&G Optoelectronics)[6] and Hamamatsu Photonics.[7] In general, the Hamamatsu devices tend to have small active thicknesses, making them both faster and less effi-

[6] Perkin–Elmer, 22001 Dumberry Rd., Vaudreuil J7V 8P7 Quebec. http://www.perkinelmer.com. Note that as the change from EG&G to Perkin–Elmer occurred as this article was going to press, we continue to refer to "EG&G" devices within the text.

[7] Hamamatsu Photonics K.K., Solid State Division, 1126-1, Ichino-cho, Hamamatsu City, 435-91 Japan. http://www.hamamatsu.com.

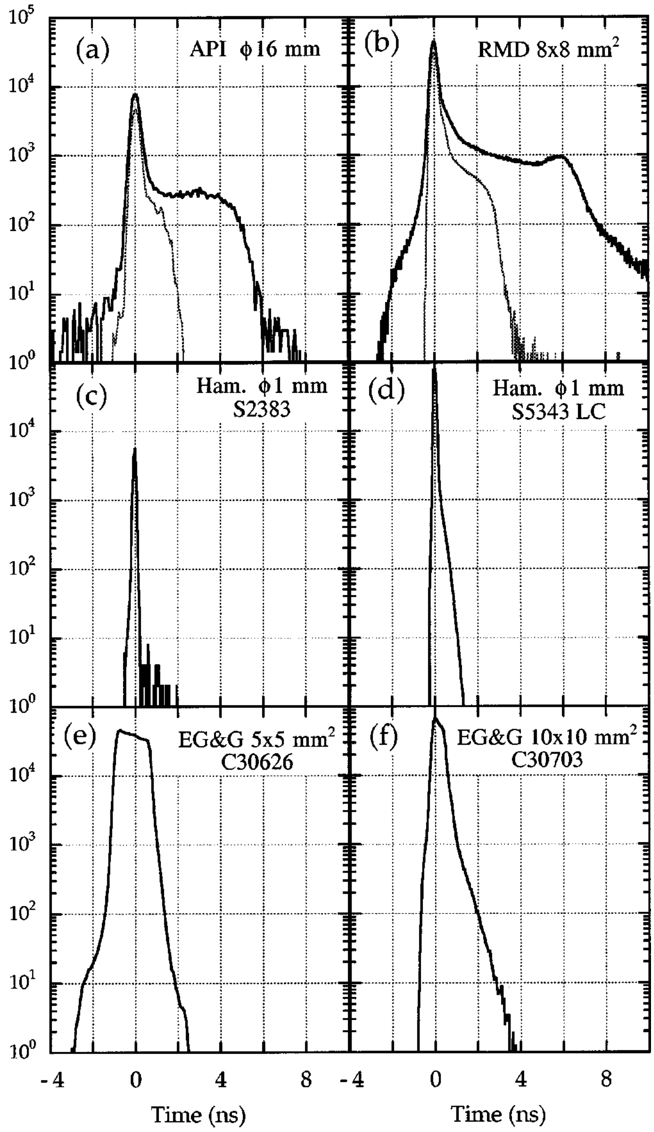

Figure 5. Time response measured using X-rays between 14 and 16 keV. Light lines in (a) and (b) show that the tail may be reduced by increasing the discriminator threshold (reducing the efficiency).

cient, while the EG&G devices tend to be thicker (more efficient), but respond more slowly. We discuss the various devices in some detail below (see also table 1). However, the reader should be aware that more devices are always being put on the market, so that one should also inquire directly of the manufacturer. We note, for example, the relatively recent appearance of a thicker device from Hamamatsu and of both a very thick device and a thin one from EG&G.

The detectors most commonly used in Europe and the US are the relatively thick reach-through devices made by EG&G. This device is based on a 120 μm thick Si wafer, with a narrow gain region located in the back of the device, so it presents, at normal incidence, an active thickness for X-ray absorption of something like 110 μm of silicon (25% efficiency at 14.4 keV). These devices are available in 5×5 mm^2 (the C30626) and 10×10 mm^2 (C30703) designs suitable for X-ray detection (see [20,21], respectively). Smaller sizes may also be purchased but are not readily available without windows. The 5×5 mm^2 devices are also available in a ceramic frame without a back, allowing diodes to be stacked, increasing the efficiency: 30% efficiency at 30 keV has been demonstrated [20]. At ESRF, the 5×5 mm^2 devices are typically used for NFS measurements while the larger area ones are used for inelastic absorption measurements. However, we note that the larger capacitance of the 10×10 mm^2 devices means that the 6.4 keV signal can be nearly in the electronic noise and, in this author's experience, only about half of the 10×10 mm^2 devices tested were well suited to 6.4 keV detection (had high enough gains). However, relative to the ⌀16 mm API devices they are extremely reliable and provide similar count rates (the smaller area of the EG&G devices compensated by enhanced efficiency). One notes, however, that the lead-time for purchasing EG&G devices can sometimes be long.

The Hamamatsu devices were the first used for X-ray timing applications [4] and, of the devices measured, they provide the best time resolution, reaching some 100 ps FWHM [22]. However, they also typically have small active thicknesses ($\sim$30 μm for the S238X series [4] and $\sim$10 μm for the S534X series [22]) and the largest size generally available is ⌀5 mm. The recently introduced SPL2625, ⌀3 mm, however, has a larger active thickness (about 120 μm [23]) and should be comparable to the $\sim$120 μm EG&G devices. It is also possible to order the SPL2625 in a transmission mount. We note, however, that this device is typically not hermetically sealed, and this author has noticed some degradation of its performance with time: of four devices tested, two showed dark current increases, making them unusable. One of these recovered on baking (24 h in a vacuum oven at 85°C).

Finally, we present some additional information that has become available during the time between the first writing of this paper and the final version for the review. EG&G will now sell their standard 10×10 mm^2 devices in a flat pack without sealing the back[8]. This allows one to make, relatively inexpensively, a transparent device which may be stacked. However, one notes these devices are moisture sensitive and may require baking before being sealed. In addition, EG&G has now produced, at least on a limited scale, some devices using a 200 μm wafer. Based on the two devices investigated by this author, they have an active thickness of about 185 μm [24] and a time resolution that is very similar to the 5×5 (626). Also notable is that the signal heights are improved (due to the lower capacitance) so 6 keV detection seems easier. Hamamatsu has also produced a "low capacitance" version of the 5343 structure. Aside from an extremely good signal-to-noise ratio, the time response seems

[8] Originally done at the request of the Hamburg Group (especially Yu.V. Shvyd'ko).

to retain many of the desirable characteristics of the S5343 response (e.g., better than 200 ps FWHM and very short tail) with a better (about 25 μm) active thickness [24].

9. APD array detectors

As NRS matures as a field, there tends to be more interest in time resolving array detectors, to cover larger areas, to reduce the load (per element) of the prompt pulse, and for position resolution. Here we mention some of the devices that have been fabricated, or are being developed, without going into great detail as arrays are not (yet) commonly used. EG&G (or RCA) has fabricated several linear arrays including a 32 element array (150 μm pitch, pixels about $50 \times 350\ \mu m^2$) [25], a 128 element array (150 μm pitch, pixels 50 μm × 2 mm) [26], and a 25 element array (300 μm pitch, pixels 250 μm × 400 μm) [27]. API has fabricated some arrays by segmenting beveled edge devices including a 3 × 3 array (pixels $3 \times 3\ mm^2$) [28] and 8 × 8 arrays (pixel size $1.3 \times 1.3\ mm^2$ [29] or 450 μm pitch [30]). Hamamatsu has also fabricated linear arrays with up to 16 channels (1.6 mm pitch for ⌀1 mm devices, or 1.1 mm pitch for $1\ mm^2$ devices) [31]. There are also arrays under development, including a 32 element array (2 rows of 16 pixels, each $3 \times 5\ mm^2$), by Kishimoto and Hamamatsu [32] and some arrays using a "planar beveled" structure by RMD [33].

10. Concluding comments

Detectors used in nuclear scattering of synchrotron radiation have undergone significant changes and improvements in the 15 years (or so) since the first successful measurements. Presently, nearly all experiments (<26 keV) are done with solid-state avalanche photodiodes: this paper has attempted to provide both an introduction to these detectors and an overview of the devices available.

Looking briefly at the present, the reliability and relative thickness of the EG&G 120 μm reach-through devices has made them the staple device in Europe and the US. The similar Hamamatsu device, while somewhat thicker, seems not yet to be so reliable and is (presently) only generally available in a smaller (3 mm) size. However, this device has only recently been introduced, and might be expected to improve. The thin Hamamatsu devices provide extremely good time resolution, with, notably, the S534X low capacitance series providing <200 ps resolution, a small tail at long times, and a modest active thickness. The use of transmission devices, allowing "stacking" of diodes to improve efficiency, is also becoming more common. However, here one should be careful about the packaging and the moisture sensitivity of the devices.

Looking into the future of APDs in nuclear scattering experiments, one can see several avenues for improvement and exploration, mostly centered on multi-element or array devices. For incoherent scattering (i.e., inelastic absorption measurements) the use of an array detector to reduce the prompt load and to increase the active area is one promising approach [32]. However, with the increasing use of non-iron isotopes, where the scattered radiation can sometimes be of higher energy (>20 keV), it may also be very interesting to consider a stacked detector of, say, two or three of the 10×10 mm^2 200 μm EG&G devices, to improve the efficiency without a large increase in complexity. In a forward scattering detector, improvements in the recovery time after the prompt pulse, the efficiency and the time resolution (especially for non-iron isotopes) would all be desirable. All of these might be accomplished by using an array of thinner devices at grazing incidence, and is an approach being considered by this author. Of course, an array device increases the complexity and expense of the electronics. While the use of a compact, inexpensive, low-power amplifier (see [20]) is a good start, it would also be desirable to integrate the discriminator as well. The nuclear (or high energy physics) data taking format is probably also worth pursuing, as the experiments where array detectors are interesting are frequently those where the count rates are relatively low.

References

[1] E. Gerdau, R. Rüffer, H. Winkler, W. Tolksdorf, C.P. Klages and J.P. Hannon, Phys. Rev. Lett. 54 (1985) 835.
[2] J. Metge, R. Rüffer and E. Gerdau, Nucl. Instrum. Methods A 292 (1990) 187.
[3] U. Bergmann, S.D. Shastri, D.P. Siddons, B.W. Batterman and J.B. Hastings, Phys. Rev. B 50 (1994) 5957;
S. Shastri, private communication (1998).
[4] S. Kishimoto, Nucl. Instrum. Methods A 309 (1991) 603 and Rev. Sci. Instrum. 63 (1992) 824.
[5] A.Q.R. Baron and S.L. Ruby, Nucl. Instrum. Methods A 343 (1993) 517.
[6] A.Q.R. Baron, Ph.D. thesis, Stanford University (1994).
[7] E. Gerdau and J. Metge, private communication (1998).
[8] R.L. Cohen, G.L. Miller and K.W. West, Phys. Rev. Lett. 41 (1978) 381.
[9] K. Quast, Diploma thesis, Universität Hamburg (1993).
[10] W. Sturhahn, K.W. Quast, T.S. Toellner, E.E. Alp, J. Metge and E. Gerdau, Phys. Rev. B 53 (1996) 171.
[11] K. Taizo, Shinkuu 41 (1998) 3 (in Japanese).
[12] U. Bergmann, J.B. Hastings and D.P. Siddons, Phys. Rev. B 49 (1994) 1513.
[13] P.P. Webb, R.J. McIntyre and J. Conradi, RCA Rev. 35 (1974) 234.
[14] S.M. Sze, *Physics of Semiconductor Devices* (Wiley, New York, 1981).
[15] C. Jacoboni, C. Canali, G. Ottaviani and A.A. Quaranta, Solid-State Electronics 20 (1977) 77.
[16] D.T. Cromer and D.A. Liberman, Acta Crystallogr. A 37 (1981) 267;
W.H. McMaster, N.K.D. Grande, J.H. Mallet and J.H. Hubbell, Compilation of X-ray cross-sections, Lawrence Radiation Laboratory (1969).
[17] S. Brennan and P.L. Cowan, Rev. Sci. Instrum. 63 (1992) 850.
[18] G.F. Knoll, *Radiation Detection and Measurement* (Wiley, New York, 1989).
[19] R. Farrell, K. Vanderpuye, L. Cirignano, M.R. Squillante and G. Entine, Nucl. Instrum. Methods A 353 (1994) 176.
[20] A.Q.R. Baron, R. Rüffer and J. Metge, Nucl. Instrum. Methods A 400 (1997) 124.
[21] A.Q.R. Baron, Nucl. Instrum. Methods A 352 (1994) 665.
[22] S. Kishimoto, Nucl. Instrum. Methods A 351 (1994) 554;
S. Kishimoto, Rev. Sci. Instrum. 66 (1995) 2314.

[23] S. Kishimoto, N. Ishizawa and T. Valasta, Rev. Sci. Instrum. 69 (1997) 384.
[24] A.Q.R. Baron et al., unpublished.
[25] M. Trakalo, P.P. Webb, P. Poirrier and R.J. McIntyre, Applied Optics 26 (1987) 3594.
[26] P.P. Webb and B. Dion, in: *SPIE Conf. on Optical Enhancements to Computing Technology* (1991) p. 236.
[27] P.P. Webb and R.J. McIntyre, IEEE Trans. Electron Dev. 31 (1994) 1206.
[28] E. Gramsch, S. Zhang, M. Madden, M. Lindberg and M. Szawlowski, in: *Conference Record of the 1992 IEEE Nuclear Science Symp. and Medical Imaging Conf.*, Cat. No. 92CH3232-6, Orlando, FL, p. 186.
[29] E. Gramsch, S. Zhang, M. Madden, M. Lindberg and M. Szawlowski, Proc. of the SPIE 2022 (1993).
[30] E. Gramsch, M. Szawlowski, S. Zhang and M. Madden, IEEE Trans. Nucl. Sci. 41 (1994) 762.
[31] K. Hara, K. Hata, T. Kikuchi, S. Kim, K. Kondo, S. Miyashita, I. Nakano, H. Okutomi, M. Sano, Y. Seiya, S. Takashima, K. Takikawa and M. Tanaka, Nucl. Instrum. Methods A 383 (1996) 252.
[32] S. Kishimoto, private communication (1998).
[33] R. Farrell (RMD), private communication (1997).
[34] M.J. Szawlowski, S. Zhang, A. DeCecco, M. Madden, M. Lindberg and E. Gramsch, in: *Conference Record of the 1992 IEEE Nuclear Science Symp. and Medical Imaging Conf.*, Cat. No. 92CH3232-6, Orlando, FL (1992) p. 239.
[35] T.S. Toellner, W. Sturhahn, E.E. Alp, P.A. Montano and M. Ramanathan, Nucl. Instrum. Methods A 350 (1994) 595.
[36] E.M. Gullikson, E. Gramsch and M. Szawlowski, Appl. Optics 34 (1995) 4662.
[37] R. Farrell, K. Vanderpuye, G. Entine and M.R. Squillante, IEEE Trans. Nucl. Sci. 38 (1991) 144.
[38] R. Farrell, K. Vanderpuye, L. Cirignano, M.R. Squillante and G. Entine, Nucl. Instrum. Methods A 353 (1994) 176.
[39] M.R. Squillante, G. Reiff and G. Entine, IEEE Trans. Nucl. Sci. 32 (1985) 563;
M.R. Squillante, R. Farrell, J.C. Lund, F. Sinclair, G. Entine and K.R. Keller, IEEE Trans. Nucl. Sci. 33 (1986) 336.
[40] J.A. Hauger, Y. Choi, A.S. Hirsch, R.P. Scharenberg, B.C. Stringfellow, M.L. Tincknell, N.T. Porile, G. Rai, J. Garbarino and R.J. McIntyre, Nucl. Instrum. Methods A 377 (1994) 362.
[41] P.P. Webb and A.R. Jones, IEEE Trans. Nucl. Sci. 21 (1974) 151;
P.P. Webb and R.J. McIntyre, IEEE Trans. Nucl. Sci. 23 (1976) 138.